Polyaniline/akaganéite superparamagnetic nanocomposite for cadmium uptake from polluted water

Azza Shokry[a],*, Ayman El Tahan[b], Hesham Ibrahim[a], Moataz Soliman[c], Shaker Ebrahim[c]

[a]*Department of Environmental Studies, Institute of Graduate Studies and Research, Alexandria University, P.O. Box: 832, 163 Horreya Avenue, El-Shatby, Alexandria, Egypt, email: azzashokry@alexu.edu.eg (A. Shokry), Tel. +201224788928; email: hz_ibrahim@yahoo.com (H. Ibrahim)*
[b]*Physics Department, Faculty of Science, Tanta University, P.O. Box: 44519, Tanta, Egypt, email: ayman.eltahan@science.tanta.edu.eg*
[c]*Department of Materials Science, Institute of Graduate Studies and Research, Alexandria University, P.O. Box: 832, Alexandria, Egypt, email: msoliman@ieee.org (M. Soliman), shaker.ebrahim@alexu.edu.eg (S. Ebrahim)*

ABSTRACT

The uptake of low concentration toxic cadmium ions from polluted water by polyaniline/akaganéite superparamagnetic nanocomposite was investigated. Akaganéite superparamagnetic nanoparticles (NPs) and polyaniline (PANI) doped with hydrochloric acid were synthesized by co-precipitation and chemical polymerization methods, respectively. Polyaniline/akaganéite superparamagnetic nanocomposite was formed using facile polymerization method. High resolution transmission microscope image of PANI/akaganéite nanocomposite revealed that it is composed of sheets of spherical shaped PANI as a matrix including nanocrystals of akaganéite NPs. These sheets have diameter ranging from 9.03 to 16.10 nm. It was noted that the hysteresis loops of akaganéite NPs and PANI/akaganéite nanocomposite shows no remanence or coercivity, suggesting a superparamagnetic property with magnetization saturation values of 45.66 and 52.73 emu g^{-1}, respectively. The effect of pH solution, initial Cd(II) concentration, nanocomposite amount and adsorption time on the efficiency of Cd(II) uptake was studied. The amount of 0.4 g L^{-1} of polyaniline/akaganéite nanocomposite was found to be sufficient to remove 94.7% from 25 ml of polluted solution of 5.0 mg L^{-1} Cd(II) ions at pH 7.0 for 5 min contact time at ambient temperature. It was observed that Langmuir maximum adsorption capacity of PANI/akaganéite nanocomposite was 33.7 mg g^{-1}.

Keywords: Superparamagnetic; Polyaniline; Iron-oxide; Akaganéite; Adsorption

1. Introduction

Superparamagnetic materials have widespread applications for the removal of heavy metal ions such as Cr(VI), As(V), Hg(II), Ag(I) and Pb(II) from aqueous solutions [1,2]. The water crisis is a result of population growth that causes rapid unsafe industrialization. It is important to remove these toxic heavy metals from water and wastewater. Cadmium is toxic and carcinogen heavy metal that damages the human physiology and the biological systems and recommended

the permissible limit of cadmium is 0.01 mg L^{-1} [3]. Various approaches have developed for the uptake of cadmium from industrial wastewater such as coagulation/precipitation, ion exchange, membrane filtration, electrodialysis, etc. Adsorption technique is one of the most separation technologies due to its naivety of design, low cost, ease of operation, sludge free operation, the potential for regeneration and high adsorption efficacy [3,4]. Nanosized iron-oxides such as hematite, akaganéite, and magnetite attract

* Corresponding author.

much attention because they can be separated from water under a magnetic field. Also, their composites adsorbents allow isolating from aqueous solution for regeneration [5,6]. Akaganéite has unique properties such as a monoclinic crystal structure, a metallic luster, and a brownish yellow color. The akaganéite structure with small tunnels has a partially chloride anion which makes it an interesting material in the removal of heavy metals [7]. Conducting polymers have popularity as adsorbents due to their simplicity of synthesis, tunable morphology, porous structure, non-toxicity, insolubility in aqueous solution and reversible ions sorption/desorption capability [8]. Polyaniline (PANI) is a conducting polymer with great potential due to its low cost, ease of preparation, good thermal and electrical properties, its environmental stabilities and versatile applications [9]. Nowadays, conducting PANI/inorganic nanocomposites have also attracted more and more attention. The properties of these nanocomposites are different from PANI and the corresponding inorganic nanoparticles (NPs) due to interfacial interactions between inorganic NPs and PANI macromolecules [10]. Due to these unique properties, PANI nanocomposites have different applications such as chemical sensors, water treatment, light-emitting diodes and electronic devices [11–13]. The main objective of this work is to remove low concentrations of Cd(II) ions in the range from 0.5 to 12.4 ppm using superparamagnetic polyaniline/akaganéite nanocomposite prepared by facile polymerization method. The prepared akaganéite NPs and nanocomposite are characterized using Fourier transform infrared (FTIR), X-ray diffraction (XRD), high-resolution transmission microscopy (HRTEM) and scanning electron microscope (SEM). Also, zeta potential and magnetization-applied magnetic field measurements are investigated for polyaniline/akaganéite nanocomposite. The effects of solution pH, initial Cd(II) concentration, nanocomposite amount and adsorption time on the removal efficiency of Cd(II) ions are studied and discussed.

2. Materials and methods

2.1. Materials

Aniline (98.5%) was obtained from El-Nasr Chemical Company (Alexandria), Egypt. HCl (36.0%) was purchased from Sigma-Aldrich (USA). Ammonium peroxydisulfate (APS) (98.0%) and methanol (HPLC grade) were received from Fisher Scientific. Acetone (99.9%) was purchased from Sigma-Aldrich (USA). Anhydrous of $FeCl_3$ (98.0%) and $FeCl_2$ (99.0%) were brought from Across Organics (USA). NaOH (98.0%) was purchased from Sigma-Aldrich (USA). Ethanol (HPLC grade) was obtained from Fisher Scientific, UK. Cadmium chloride (99.0%) was obtained from Merck (Germany).

2.2. Polyaniline synthesis

Polyaniline doped with HCl (emeraldine salt) was synthesized by chemical polymerization of aniline in an aqueous acidic solution. 40 ml of aniline was dissolved in precooled (5°C) 1 M hydrochloric acid, and 27 g of APS was also dissolved in precooled (5°C) 1 M hydrochloric acid. The APS solution was then added dropwise through 1 h to aniline solution and the mixture was preserved for 24 h

with continuous stirring at 5°C to confirm the completion of polymerization. Polyaniline-hydrochloride green powder was collected on a filter paper by a vacuum and washed with deionized water, methanol, and acetone, respectively until the filtrate solution becomes colorless and finally the powder of emeraldine salt was dried at ambient temperature for 48 h.

2.3. Synthesis of akaganéite NPs

The co-precipitation method was used to synthesis akaganéite NPs. Ferric chloride (1.275 g) and 3.121 g of ferrous chloride were mixed and dissolved in 25 ml 0.4 M HCl. This mixture was added slowly through 1 h into 250 ml of 1.5 M NaOH with vigorous stirring under N_2 gas. The formed precipitate in NaOH solution was heated at 75°C for 30 min and was separated using a magnet, washed with deionized water and ethanol, respectively. The akaganéite NPs powder formed was dried at room temperature.

2.4. Synthesis of polyaniline/akaganéite nanocomposite

PANI/akaganéite nanocomposite with NPs loading of 30 wt.% was prepared by surface-initiated polymerization method. A mixture of 1.44 g akaganéite NPs, 18.0 mmol APS and 30.0 mmol HCl were added into 200.0 ml deionized water in an ice-water bath for 1 h with vigorous stirring. Then, 36.0 mmol in 50.0 ml deionized water of aniline aqueous solution was mixed with the above akaganéite NPs suspension and stirred continuously for 24 h in an ice-water bath for further polymerization. The product was vacuum filtered on a filter paper, washed with deionized water until the pH was approximately 7.0 and further washed with methanol to remove any possible oligomers and the final nanocomposite powder was dried.

2.5. Characterization techniques

The crystallinity of the prepared nanocomposite was evaluated by XRD using (X-ray 7000 Shimadzu-Japan). The Cu target of the X-ray source was generated at 30 kV and 30 mA with a scan speed of 4 deg min^{-1}. FTIR spectrophotometer (Spectrum BX 11- LX 18–5255 Perkin Elmer, USA) was used to identify the main functional groups of PANI/akaganéite nanocomposite. The samples were mixed and ground with dried potassium bromide and pressed under high pressure. The IR spectra were recorded in a wavenumber range of 4,000–350 cm^{-1}. The morphology of PANI/akaganéite nanocomposite was characterized by (SEM "JEOL JSM-5300", Japan). The sample was used in the powder form and was coated with a sputtered gold layer. Particle size was studied using HRTEM (JEM-2100, Japan). HRTEM sample was prepared by dispersing 2 mg of the nanocomposite powder in 5 ml of ethanol and sonicated. A drop of this solution was evaporated on a copper grid and tested. Magnetization vs. applied magnetic field (M–H) hysteresis loops for akaganéite NPs and nanocomposite samples packed in the calibrated Teflon sample holder were obtained at room temperature by vibrating sample magnetometer (VSM, Lake Shore Cryotronics, Inc., Ohio, USA). Finally, the charges onto akaganéite NPs and PANI/akaganéite nanocomposite were measured using a Zetasizer Malvern Nano-ZS (UK).

The suspension was placed in a universal folded capillary cell attached to platinum electrodes.

2.6. Uptake of Cd(II) ions onto PANI/akaganéite nanocomposite surface

A stock solution of 1,000 mg L^{-1} of Cd(II) ions was prepared by an dissolving appropriate amount of cadmium chloride in deionized water. Cd(II) solutions with the required concentration were freshly diluted from this stock solution. Different experiments were performed by mixing 10 mg (equivalent to 0.4 g L^{-1}) of PANI/akaganéite nanocomposite with 25 ml of Cd(II) ions in aqueous solutions. These mixtures were continuously stirred for 5 min under sonication. The adsorbent was separated from Cd(II) solutions by using a magnet. Then these solutions were analyzed by the atomic absorption spectrophotometer (Sens AA, GBC Dual). The pH of Cd(II) solutions was adjusted by 1 M NaOH and 1 M HCl with a pH meter (Martini MI150 pH/temperature Bench Meter, USA). The removal percentage (*R*%) and capacity (*Q*, mg g^{-1}) of Cd(II) were calculated according to the equations in the previous publication [12].

2.7. Desorption and reusability

The regenerability and reusability of PANI/akaganéite nanocomposite after Cd(II) adsorption was investigated by adsorption–desorption experiments. Sample of 10.0 mg (equivalent to 0.4 g L^{-1}) of the nanocomposite was used to remove 5.0 mg L^{-1} Cd(II) ions from 25 ml solution at pH 7.0 for 5 min at room temperature. For Cd(II) desorption, the Cd(II) loaded adsorbent was mixed with 25 ml of HCl (1 M) solution under sonication for 15 min to remove the adsorbed Cd(II) ions [14]. Cadmium concentration in the solution was determined. Desorption efficiency (%) was calculated using the following equation [15]:

$$\text{Desorption}(\%) = \frac{\text{Released metal concentration to solution}(\text{mg}/\text{L})}{\text{Total adsorbed metal concentration}(\text{mg}/\text{L})} \times 100 \tag{1}$$
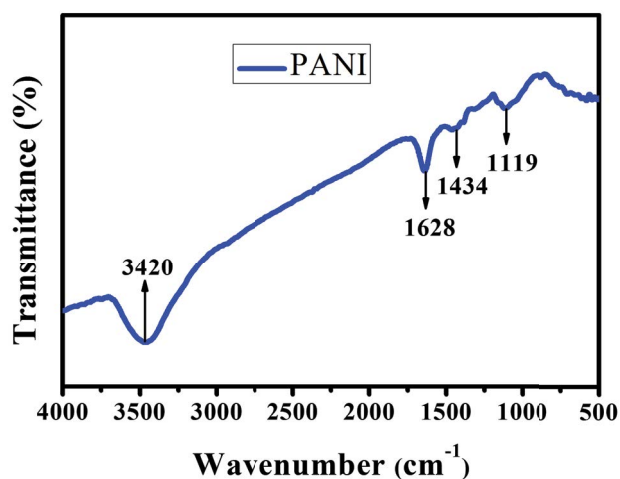
The used nanocomposite powder was washed with deionized water until the pH was approximately 7.0. Then the sample was dried at 50°C overnight. The regenerated sample was used again to treat a 25 ml solution with Cd(II) concentration of 5.0 mg L^{-1}.

3. Results and discussion

3.1. Structural and morphological properties of PANI/akaganéite nanocomposite

Fig. 1 depicts FTIR spectra of PANI and the PANI/akaganéite nanocomposite before and after treatment with Cd(II) solution. The adsorption band at 1,136 cm^{-1} is attributed to the vibration of the –NH^+ groups formed in the acid doping process of polyaniline of PANI/akaganéite nanocomposite [16]. Bands at 1,510 and 1,603 cm^{-1} are assigned to the stretching of the benzenoid and quinoid rings, respectively in PANI/akaganéite nanocomposite [12,17]. Also, the band at 3,431 cm^{-1} represents the N–H stretching mode of PANI/akaganéite nanocomposite [12,17]. The characteristic peak at 578 cm^{-1} is attributing to the Fe–O stretching band of iron-oxide NPs in PANI/akaganéite nanocomposite [4,18]. The major changes in the IR spectra between treated and untreated PANI/akaganéite nanocomposite are observed in the bands corresponding to absorption peaks of quinoid and benzenoid rings. After the adsorption of Cd(II) ions by PANI/akaganéite nanocomposite, the absorption peaks corresponded to the imine, amine and protonated amine groups have been shifted from 1,603; 1,510; and 1,136 cm^{-1} to 1,622 cm^{-1}, 1,504 cm^{-1}, and 1,126 cm^{-1}. This is due to the interaction between imine, amine and protonated imine groups and cadmium ions during the adsorption process [4].

The XRD pattern of PANI/akaganéite nanocomposite is shown in Fig. 2. The main characteristic peaks of akaganéite (β-FeOOH) at 2θ = 12.3° and 27.2° are indexed to (110) and (310), respectively. Also, a small fraction of hematite appears at 2θ = 24.7° corresponding to (012) (JCPDS No. 89–0597) [12]. These results indicate that iron-oxide NPs consist of akaganéite phase which is the main component with a small ratio of hematite phase.
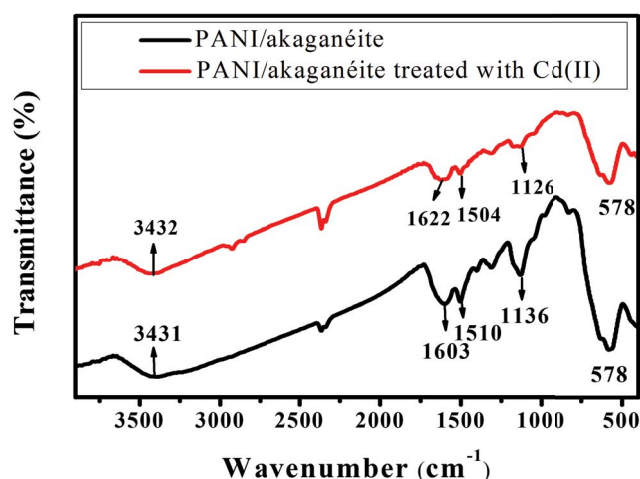

Fig. 1. FTIR spectra of PANI and PANI/akaganéite nanocomposite before and after treated with Cd(II).
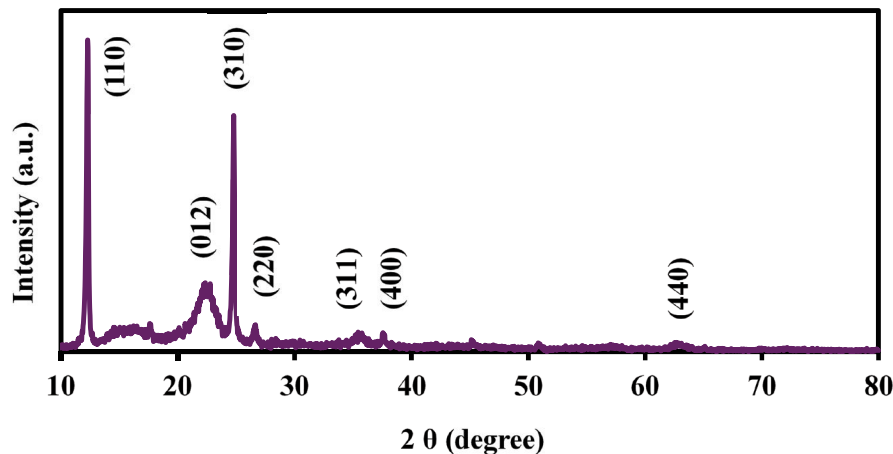
Fig. 2. XRD pattern of PANI/akaganéite nanocomposite.

Fig. 3 illustrates SEM and TEM microstructures of PANI/akaganéite nanocomposite. As observed in Fig. 3a, SEM image shows a cauliflower structure. It is noted that there is no appearance for the akaganéite NPs suggesting that polymerization of polyaniline occurred on the surface of the akaganéite NPs. The HRTEM image of PANI/akaganéite nanocomposite shown in Fig. 3b reveals that the nanocomposite is composed of sheets of spherical shaped PANI as a matrix including nanocrystals of akaganéite NPs. These sheets have a diameter ranging from 9.03 nm to 16.10 nm.

3.2. Magnetic properties of akaganéite NPs and PANI/akaganéite nanocomposite

The magnetic properties of the prepared akaganéite NPs and PANI/akaganéite nanocomposite were studied by VSM at room temperature. The plots of magnetization (M) vs. the magnetic field (H) (M-H loop) are given in Fig. 4. A great difference between bulk magnetic materials and NPs is that the magnetization direction is unstable in magnetic NPs because

the thermal energy can adequate to overcome the energy barrier separating the directions of magnetization. It is noted that the hysteresis loops of akaganéite NPs and PANI/akaganéite nanocomposite shows no remanence or coercivity, suggesting a superparamagnetic property with magnetization saturation values of 45.66 and 52.73 emu g^{-1}, respectively. These magnetization values are high enough to separate the akaganéite NPs and nanocomposite from the aqueous solution because magnetization of 16.3 emu g^{-1} is sufficient to magnetic separation with a permanent magnet [19].

3.3. Effect of solution pH on Cd(II) adsorption

The pH of the solution was considered as one of the most important parameters controlling the metal adsorption. This is attributed to the fact that the pH of the solution significantly influences the surface charge characteristics of the adsorbents [20,21]. Effect of pH on both R and Q for 5.0 mg L^{-1} Cd(II) solution after treatment with 0.4 g L^{-1} of nanocomposite for 5 min at room temperature is illustrated
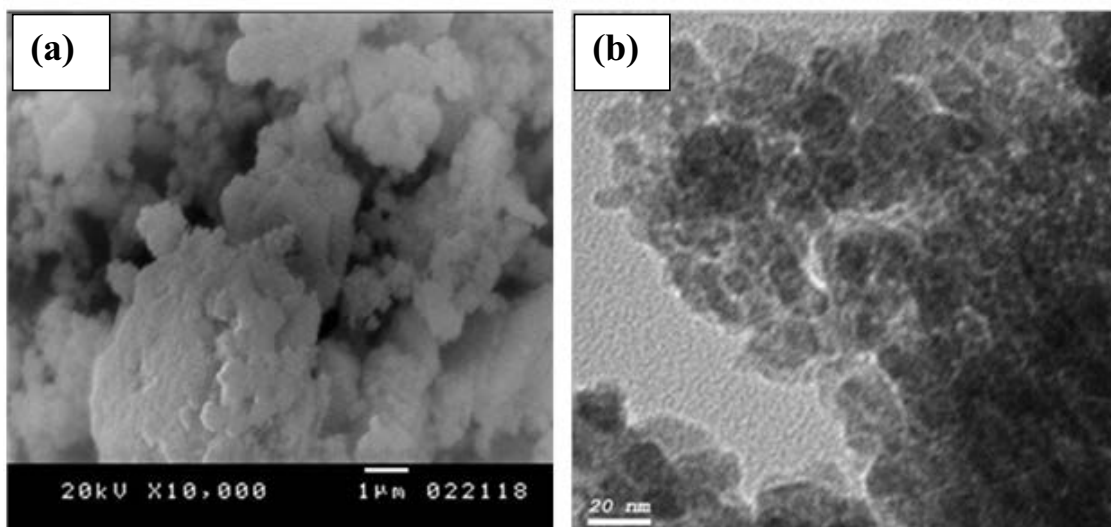

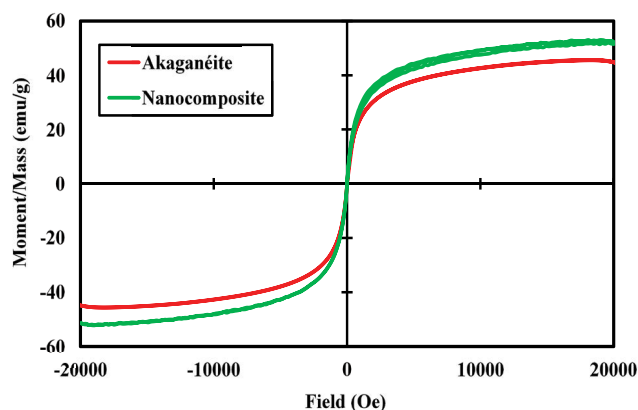Fig. 3. (a) SEM and (b) HRTEM images of PANI/akaganéite nanocomposite.

Fig. 4. M–H plots of akaganéite NPs and PANI/akaganéite nanocomposite.

in Fig. 5. It is observed that at pH higher than 7.0, Cd(II) ions precipitation as hydroxides is occurred [22]. *R* of Cd(II) ions is increased from 50.6% to 94.7% by increasing the pH of the solution from pH 4.0 to pH 7.0. Similarly, the *Q* value is raised from 6.33 to 11.84 mg g^{-1} by elevating the solutions pH from pH 4.0 to pH 7.0, respectively [20,23,24]. Cadmium can be found in different forms depending on the pH of the solution. At pH < 8.0, the main form is Cd(II) and its removal occurs mainly via adsorption reactions [20]. In an acidic medium, at low pH, the concentration of protons (H$^+$) is much higher than of the Cd(II) ions. Therefore, there are competition between H$^+$ ions and Cd(II) ions due to the repulsive force on the polyaniline surface, and Cd(II) ions hindered from reaching the adsorbent binding sites because of this repulsive force [21,25,26]. Also, the electrostatic repulsion between the Cd(II) ions and the positive charge on the surface of polyaniline is increased. These effects result in the reduction of Cd(II) ions adsorption at low pH. In the meantime, the surface of akaganéite NPs is also positively charged at low pH and cadmium ions cannot be adsorbed
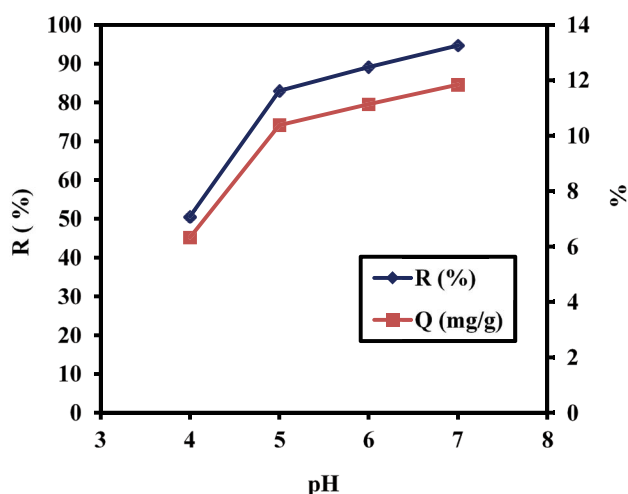
onto iron-oxide NPs due to repulsive force between the positively charged surface of akaganéite NPs and Cd(II) ions [27]. With the increase of the solution pH, the positive charge on the surface of the polyaniline is decreased and the adsorption of Cd(II) ions through the electrostatic attraction may be increased [28]. At pH 7.0, multiple adsorption sites consisting of imine (–N=), amine (NH–) and protonated imine (–NH$^+$–) are coexisted. These sites could be further subcategorized into type-one (imine) and type-two (amine and protonated imine) sites, with type-one sites having higher a affinity to cadmium than type-two sites [29]. The proposed mechanism describing the adsorption of Cd(II) by the prepared PANI/akaganéite nanocomposite is attributed to electrostatic attraction followed by chelation between Cd(II) ions and imine, amine and protonated imine groups of the PANI [30].

The surface charge plays a significant role in colloidal stability. These charges can be measured as an electrical potential in the interfacial double layer on the surface of NPs in suspension. A high zeta potential (+ or −) value is an indication of the dispersion stability of NPs due to electrostatic interaction. From the data of the zeta potential of akaganéite NPs and PANI/akaganéite nanocomposite shown in Fig. 6, the surface charge signs on the superparamagnetic NPs and nanocomposites in aqueous solutions of pH 7.0 are negative. Zeta potential values of akaganéite NPs and PANI/akaganéite nanocomposite are –17.8 and –26.4 mV, respectively, which indicate the existence of electrostatic attraction between the adsorbents surface and the metal ions. A similar kind of mechanism was reported for mercury and cadmium ions [29–32].

3.4. Effect of initial Cd(II) concentration on Cd(II) adsorption

The effect of initial Cd(II) concentration from 0.5 to 12.4 mg L^{-1} for 5 min contact time on the Cd(II) *R* and *Q* are investigated at pH 7.0 using 0.4 g L^{-1} of PANI/akaganéite nanocomposite as depicted in Fig. 7. The results demonstrate that *R* of Cd(II) ions is decreased with increasing of the initial Cd(II) concentration from 0.5 to 3.3 mg L^{-1}. The adsorbents have a fixed number of active sites and at higher Cd(II) concentrations, the active sites become saturated. However, as the Cd(II) concentration is increased further from 3.3 to 5.0 mg L^{-1}, the percentage of removal from 87.8% to 94.7% is enhanced. This is due to the driving force resulted in the concentration gradient overcome resistance to mass transfer of Cd(II) ions between the aqueous phase and the solid phase [33,34]. Further increasing Cd(II) concentration to 12.4 mg L^{-1}, the *R*-value reduces to 83.35% due to the diminishing of the available active sites for the adsorption process [24,33]. The *Q* values are linearly increased from 1.16 to 25.82 mg g^{-1} with the increasing of the Cd(II) concentration from 0.5 to 12.4 mg L^{-1}. This is attributed to the enhancement of the driving force at higher concentrations [22,25,35].

3.5. Adsorption isotherms

The adsorption isotherms are required to evaluate the adsorption behavior or interactions between adsorbent and adsorbates. Langmuir and Freundlich's isotherms are

Fig. 5. R and Q vs. pH of 0.4 g L^{-1} PANI/akaganéite nanocomposite with 25 ml of 5.0 mg L^{-1} Cd(II) solution.
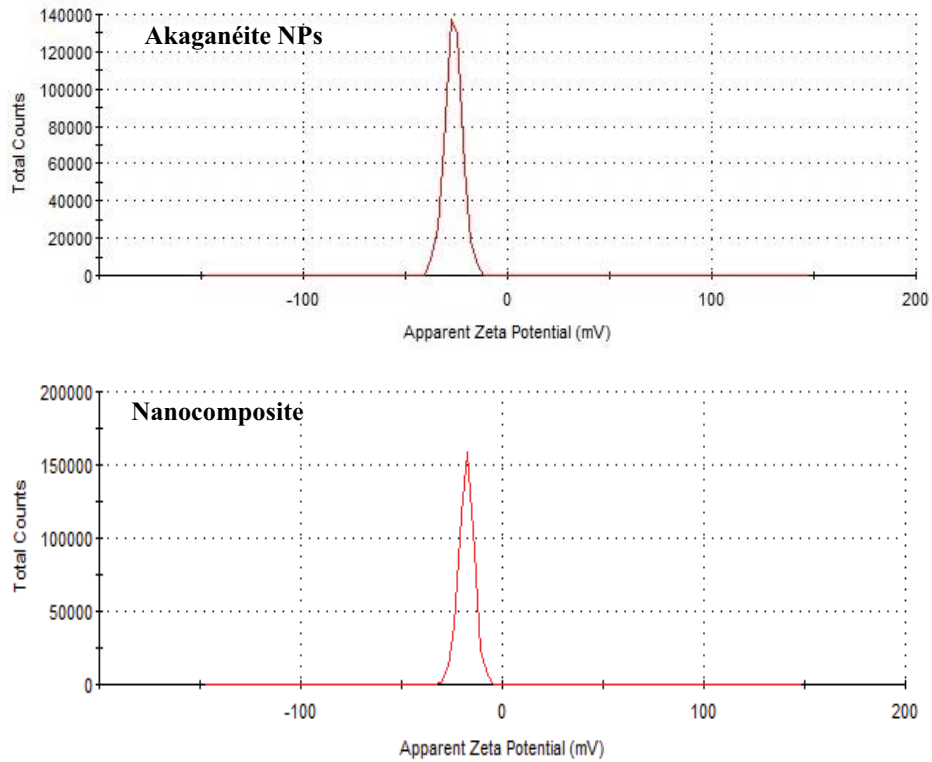
Fig. 6. Zeta potential charts of akaganéite NPs and PANI/akaganéite nanocomposite.
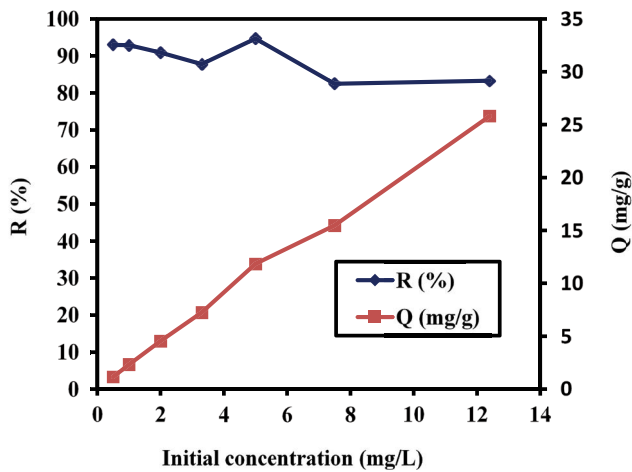

Fig. 7. R and Q vs. initial Cd(II) concentration in 25 ml Cd(II) solution with 0.4 g L^{-1} PANI/akaganéite nanocomposite.

frequently used to evaluate the adsorption behavior using Eqs. (2) and (3), respectively [36].

$$\frac{C_e}{q_e} = \frac{1}{q_m K_L} + \frac{1}{q_m} C_e \tag{2}$$

$$\log q_e = \log K_f + \frac{1}{n} \log C_e \tag{3}$$

where C_e (mg L^{-1}) is the Cd(II) concentration at equilibrium, q_e (mg g^{-1}) is the amount of metal adsorbed per unit of the adsorbent at equilibrium, K_L (L mg^{-1}) is the adsorption constant of the Langmuir model and is directly related to the binding energy of the adsorption and q_m is the maximum adsorption capacity (mg g^{-1}), K_f (mg g^{-1}(L mg^{-1})$^{-1/n}$) is Freundlich constant and n is the heterogeneity factor.

The experimental data are simulated using these two models as presented in Fig. 8. As clearly shown, the results are more fitted to the Freundlich model which is confirmed by the higher determination coefficient ($R^2 = 0.9236$). It suggests that Cd(II) ions adsorption onto PANI/akaganéite nanocomposite is a multilayer coverage [37]. The maximum adsorption capacity (q_m) of the PANI/akaganéite nanocomposite is 33.67 mg g^{-1}. The adsorption capacity of synthesized nanocomposites as compared to other available adsorbents as presented in Table 1. It is noted that PANI/akaganéite nanocomposite has the highest capacity at pH 7.0 compared to the published data.

3.6. Effect of adsorbent dose on Cd(II) adsorption

To evaluate the optimum amount of PANI/akaganéite nanocomposite, different amounts of the nanocomposite were added to 25 ml of Cd(II) solution of the initial concentration of 5.0 mg L^{-1} at pH 7.0 for 5 min at room temperature. Fig. 9 displays the effect of adsorbent dose of PANI/akaganéite nanocomposite on both R and Q of for Cd(II) solution. At the beginning, the R is increased from 89.4% to 94.8% with an increase in the amount of PANI/akaganéite
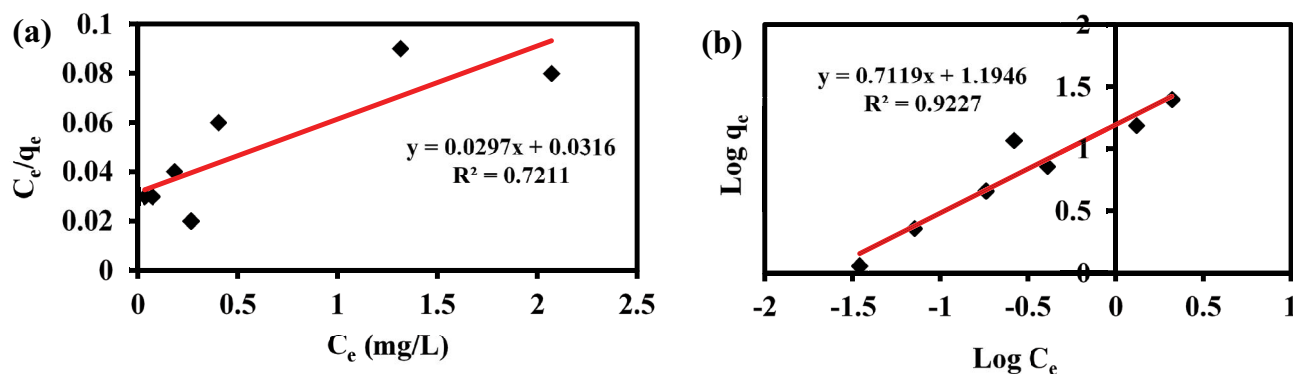
(a)

(b)

Fig. 8. Plots of (a) Langmuir isotherm and (b) Freundlich isotherm for the adsorption of Cd(II) ions onto PANI/akaganéite nanocomposite.

Table 1
Comparative adsorption capacity of various adsorbents for Cd(II) removal from aqueous solution

Adsorbents	pH	q_m (mg g^{-1})	References
Maghemite-magnetite NPs	9.3	2.7	[38]
Magnetic oak wood char	5.0	3.0	[39]
Magnetic oak bark char	5.0	7.3	[39]
Carbon F-400	5.0	8.0	[40]
Magnesium-AC composite	5.3	10.6	[41]
Nano-TiO$_2$	9.0	15.3	[42]
Carbon aerogel	6.5	15.5	[43]
Shellac-coated magnetic NPs	6.0	18.8	[44]
Magnetic ChNTs	5.5	23.8	[45]
PANI/akaganéite nanocomposite	7.0	33.7	present study

Fig. 9. R and Q vs. amount of nanocomposite in 25 ml of 5.0 mg L^{-1} Cd(II) solution at pH 7.0 for 5 min.

nanocomposite from 0.1 to 0.6 g L^{-1}, respectively. This is followed by a slight decrease as the dose increases from 0.6 to 0.8 g L^{-1} (94.8% to 92.0%, respectively). The increase in the adsorption at the beginning is attributed to the presence of more binding sites on the surface of the nanocomposite to chelate Cd(II) ions from the solution [46–48]. However, the maximum adsorption occurs at 0.4 g L^{-1} (94.7%). The Q value is decreased exponentially from 44.71 to 5.75 mg g^{-1} with increasing the amount of PANI/akaganéite nanocomposite from 0.1 to 0.8 g L^{-1}. This declined is attributed to the inter-ference between binding active sites and higher adsorbed dose. Moreover, the declined of the adsorption capacity is due to the aggregation resulting from the high sorbent dose and this leads to a decrease in total surface area of the adsorbent. The particle interaction at higher adsorbent con-centration also helps to desorbs some of the loosely bound Cd(II) ions from the adsorbent [12,28].

3.7. Effect of contact time on Cd(II) adsorption

The effect of contact time on R and Q of 5.0 mg L^{-1} of 25 ml Cd(II) solutions using 0.4 g L^{-1} of PANI/akaganéite nanocomposite is shown in Fig. 10. Results indicate that
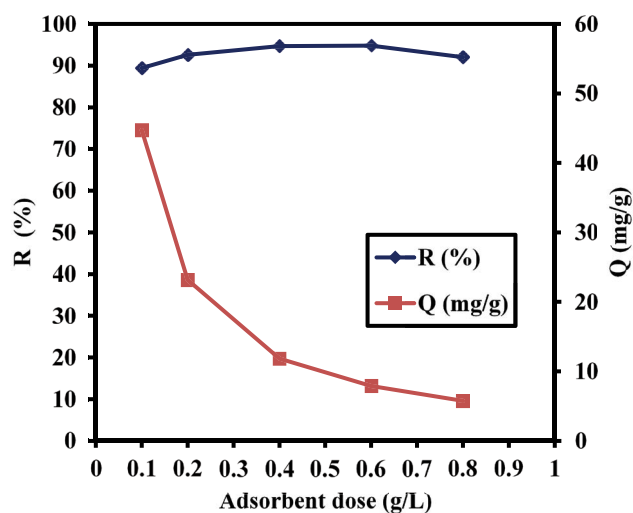
by increasing the contact time from 2 to 10 min, R of Cd(II) ions is slightly increased from 89.9% to 91.7% and the maxi-mum R of 94.7% is obtained at 5 min. These results revealed that uptake of Cd(II) ions by PANI/akaganéite nanocom-posite is fast due to the abundant binding sites on the sur-face of the adsorbent and the high affinity between Cd(II) and the adsorbent [36,49]. With the gradual occupancy of these active sites after 5 min, the nanocomposite becomes less efficient, which may be attributed to the occupancy of the whole active sites by Cd(II) ions followed by the subse-quent adsorption and desorption processes [33,34]. On the other hand, the Q of Cd(II) ions is slightly increased from 11.24 to 11.84 mg g^{-1} with rising the contact time from 2 to 5 min and the maximum removal capacity of 11.84 mg g^{-1} is attained at a contact time of 5 min.

3.8. Adsorption kinetics

The rating mechanism of Cd(II) adsorption onto PANI/akaganéite nanocomposite is studied by applying kinetic
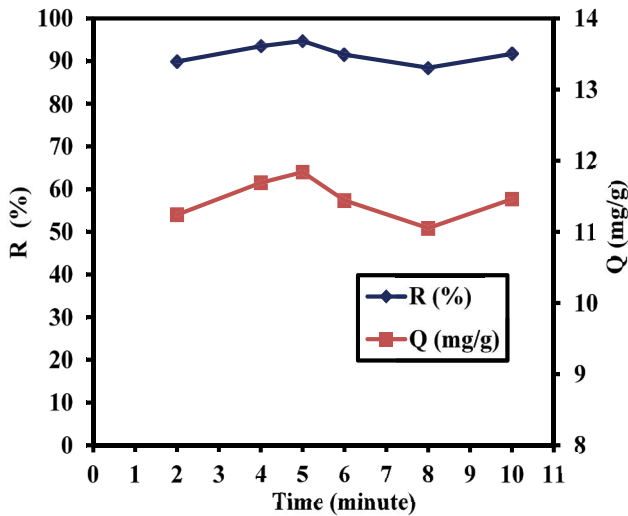
Fig. 10. *R* and *Q* vs. contact time of 0.4 g L^{-1} PANI/akaganéite nanocomposite with 25 ml of 5.0 mg L^{-1} Cd(II) solution.

models. Pseudo-first and second-order models are applied to the experimental data obtained at various contact times (2–10 min). Pseudo-first and second-order kinetic models in the linear form are expressed according to the following equations respectively [50,51].

$$\log\left(q_e - q_t\right) = \log q_e - \frac{k_1}{2.303}t \qquad (4)$$

$$\frac{t}{q_t} = \frac{1}{k_2 q_e^2} + \frac{1}{q_e}t \qquad (5)$$

where q_e and q_t (mg g^{-1}) are the amounts of Cd(II) adsorption at equilibrium time and at contact time t, respectively. k_1 (min^{-1}) is the pseudo-first-order rate constant and k_2 (g mg^{-1} min^{-1}) is the pseudo-second-order rate constant. The values of k_1, q_e, and R^2 in the pseudo-first-order model are determined from the linear plot between log ($q_e - q_t$) and t (Fig. 11a). Similarly, the values of k_2, q_e, and R^2 in the

pseudo-second-order are calculated from the linear plot between t/q_t and t (Fig. 11b) and the kinetic parameters of the two models are given in Table 2. According to obtained results, the values of q_e (cal) (11.56 mg g^{-1}) in pseudo-second-order almost similar to q_e (exp) (11.84 mg g^{-1}) and the value of correlation coefficient of $R^2 = 0.995$ is observed (Table 1). Therefore, the pseudo-second-order model is best adapted to Cd(II) adsorption data. It is suggested the Cd(II) adsorption on the surface active sites of adsorbents controlled by chemisorptions via complexation or chelation [37,52].

3.9. Desorption and reusability of PANI/akaganéite nanocomposite

Desorption and regeneration performance of PANI/akaganéite nanocomposite after Cd(II) ions adsorption for further reuse are investigated. 10 mg of the nanocomposite already treated with initial Cd(II) concentration of 5.0 mg L^{-1} are resuspended in 25 ml of HCl (1 M) solutions under sonication for 15 min to remove the adsorbed Cd(II) ions. After removing the nanocomposite from the HCl solution, the concentration of Cd(II) ions in the HCl solution is determined. Only 0.15 mg L^{-1} of Cd(II) ions are desorbed with a desorption efficiency of 3.2%. To investigate the reusability of the adsorbents, the regenerated sample is used to treat solutions with an initial Cd(II) concentration of 5.0 mg L^{-1} at pH 7.0. Results revealed that PANI/akaganéite nanocomposite can be regenerated and reused with a removal efficiency of 90.6% for the Cd(II) ions, with 4.1% less than the unused one (94.7%).

3.10. Effect of adsorbent type on Cd(II) adsorption

The *R* values are compared and investigated using different adsorbents. These adsorbents are akaganéite NPs, PANI salt, and PANI/akaganéite nanocomposite. Doses of 0.4 g L^{-1} of each adsorbent were used to treat 25 ml solutions of an initial Cd(II) concentration of 5.0 mg L^{-1} at pH 7.0 for 5 min at room temperature (Fig. 12). It is found that PANI/akaganéite nanocomposite and akaganéite NPs exhibit removal efficiency for Cd(II) ions of 94.7% and 92.8%, respectively. On the other hand, PANI depicts the lowest removal value (48%). The dopant (Cl$^-$) ions may be partially developed from PANI
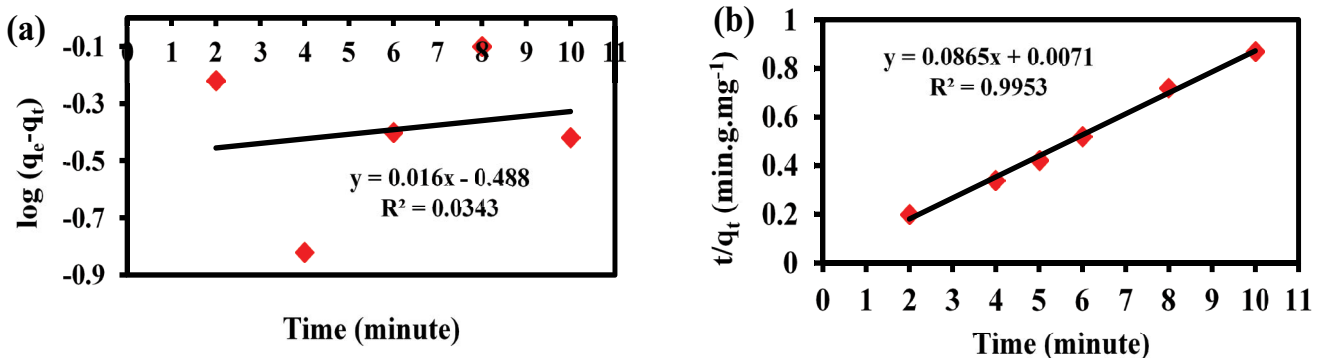

Fig. 11. Fitting of Cd(II) ion adsorption data onto PANI/akaganéite nanocomposite to (a) pseudo-first-order and (b) pseudo-second-order kinetic models.

Table 2
Kinetic parameters of pseudo-first-order and pseudo-second-order models for the adsorption of 5.0 mg L^{-1} Cd(II) ions onto PANI/akaganéite nanocomposite

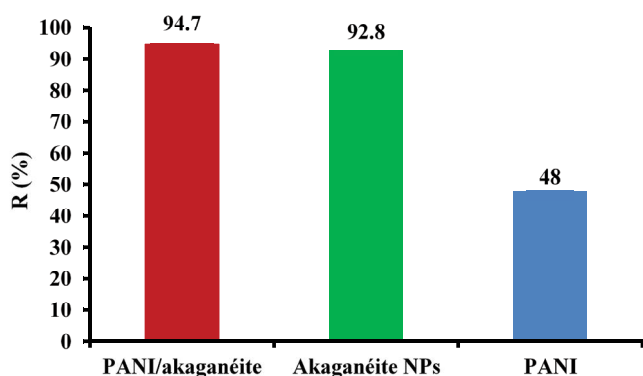| Adsorption kinetics rate models	Kinetic parameters
Pseudo-first-order model	$q_{e,exp}$ = 11.84 (mg g^{-1})
	k_1 = 0.04 (min^{-1})
	q_e = 0.33 (mg g^{-1})
	R^2 = 0.034
Pseudo-second-order model	k_2 = 1.05 (g mg^{-1} min^{-1})
	q_e = 11.56 (mg g^{-1})
	R^2 = 0.995

Fig. 12. R of Cd(II) solutions (5.0 mg L^{-1}) using different adsorbents at pH 7.0 after 5 min.

matrix, which could change the distribution of Cd(II) species by competing with OH$^-$ to form cadmium complexes such as Cd–Cl, that have lower affinity to the binding sites than Cd–OH complexes, causing lower Cd(II) removal. Similar results have been reported for the impact of Cl$^-$ on mercury sorption by polyaniline [28].

3.11. Adsorption in wastewater

The applicability of PANI/akaganéite nanocomposite for Cd(II) adsorption from wastewater is tested with an industrial wastewater sample of a leather tanning company in Alexandria. The wastewater sample is originally contaminated with 0.05 mg L^{-1} of Cd(II) ions and is spiked with 5.0 mg L^{-1} of Cd(II) to have a total of 5.05 mg L^{-1} of Cd(II) ions. A volume of 25 ml of this sample is mixed with 10.0 mg (0.4 g L^{-1}) of the nanocomposite under sonication at pH 7.0 for 5 min at room temperature. There is no obvious removal for Cd(II) ions from the wastewater sample. This is maybe because wastewater contains a significant amount of cations and anions. The presence of these ions often indicates potential competition for active adsorption sites of the adsorbents, and thus might prevent the adsorption of Cd(II) [53]. So, further studies are required to evaluate the potential PANI/akaganéite nanocomposite in the removal of Cd(II) ions from industrial wastewater.

4. Conclusions

Polyaniline/akaganéite superparamagnetic nanocomposite was synthesized by surface-initiated polymerization method and applied as an effective adsorbent for Cd(II) ions from aqueous solution. The hysteresis loops of akaganéite NPs and PANI/akaganéite nanocomposite appeared no remanence or coercivity, suggesting a superparamagnetic property with magnetization saturation values of 45.66 and 52.73 emu g^{-1}, respectively. This nanocomposite was rapidly and efficiently removed Cd(II) from aqueous solutions. Cadmium(II) removal results suggested that adsorption of Cd(II) by PANI/akaganéite nanocomposite from aqueous solution was increased with the increase of the solution pH and the maximum removal percentage (94.7%) was obtained at pH 7.0, 0.4 g L^{-1} of the superparamagnetic nanocomposite and at 5 min contact time. Both Langmuir and Freundlich isotherms were applied to study the adsorptive behavior of the nanocomposite and the best fit was obtained with the Freundlich model. Moreover, the kinetic parameters were also analyzed using the pseudo-first and second-order models. The pseudo-second-order model was the best fitted to Cd(II) adsorption.

References

[1] S.G. Lanas, M. Valiente, M. Tolazzi, A. Melchior, Thermodynamics of Hg^{2+} and Ag$^+$ adsorption by 3-mercaptopropionic acid-functionalized superparamagnetic iron oxide nanoparticles, J. Therm. Anal. Calorim., 136 (2019) 1153–1162.

[2] C.W. Kim, S.S. Lee, B.J. Lafferty, D.E. Giammar, J.D. Fortner, Engineered superparamagnetic nanomaterials for arsenic(V) and chromium(VI) sorption and separation: quantifying the role of organic surface coatings, Environ. Sci.: Nano, 5 (2018) 556–563.

[3] J. Gómez-Pastora, E. Bringas, I. Ortiz, Recent progress and future challenges on the use of high performance magnetic nano-adsorbents in environmental applications: a review, Eng. J., 256 (2014) 187–204.

[4] W. Wang, K. Cai, X.F. Wu, X.H. Shao, X.J. Yang, A novel poly (m-phenylenediamine)/reduced graphene oxide/nickel ferrite magnetic adsorbent with excellent removal ability of dyes and Cr(VI), J. Alloys Compd., 722 (2017) 532–543.

[5] Y.-X. Zhang, Y. Jia, A facile solution approach for the synthesis of akaganeite (β-FeOOH) nanorods and their ion-exchange mechanism toward As(V) ions, Appl. Surf. Sci., 290 (2014) 102–106.

[6] M. Kumari, C.U. Pittman Jr., D. Mohan, Heavy metals [chromium(VI) and lead(II)] removal from water using mesoporous magnetite (Fe$_3$O$_4$) nanospheres, J. Colloid Interface Sci., 442 (2015) 120–132.

[7] J.H. Zhao, W. Lin, Q.G. Chang, W.P. Li, Y.P. Lai, Adsorptive characteristics of akaganeite and its environmental applications: a review, Environ. Technol. Rev., 1 (2012) 114–126.

[8] M. Ayad, G. El-Hefnawy, S. Zaghlol, Facile synthesis of polyaniline nanoparticles; its adsorption behavior, Chem. Eng. J., 217 (2013) 460–465.

[9] Sh.M. Ebrahim, A.B. Kashyout, M.M. Soliman, Electrical and structural properties of polyaniline/cellulose triacetate blend films, J. Polym. Res., 14 (2007) 423–429.

[10] M. Babazadeh, F. Zalloi, A. Olad, Fabrication of conductive polyaniline nanocomposites based on silica nanoparticles via *in-situ* chemical oxidative polymerization technique, Synth. React. Inorg. Met.-Org. Chem., 45 (2015) 86–91.

[11] S. Ebrahim, R. El-Raey, A. Hefnawy, H. Ibrahim, M. Soliman, T.M. Abdel-Fattah, Electrochemical sensor based on polyaniline nanofibers/single wall carbon nanotubes composite for detection of malathion, Synth. Met., 190 (2014) 13–19.

[12] S. Ebrahim, A. Shokry, H. Ibrahim, M. Soliman, Polyaniline/akaganéite nanocomposite for detoxification of noxious Cr(VI) from aquatic environment, J. Polym. Res., 23 (2016) 79–85.

[13] S. Panda, B. Acharya, Electronic Applications of Conducting Polymer Nanocomposites, V. Nath, J. Mandal, Eds., Proceedings of the Third International Conference on Microelectronics, Computing and Communication Systems, Lecture Notes in Electrical Engineering, Springer, Singapore, Vol. 556, 2019, pp. 211–220.

[14] Q. Yuan, N. Li, Y. Chi, W.C. Geng, W.F. Yan, Y. Zhao, X.T. Li, B. Dong, Effect of large pore size of multifunctional mesoporous microsphere on removal of heavy metal ions, J. Hazard. Mater., 254–255 (2013) 157–165.

[15] R.J. Li, L.F. Liu, F.L. Yang, Preparation of polyaniline/reduced graphene oxide nanocomposite and its application in adsorption of aqueous Hg(II), Chem. Eng. J., 229 (2013) 460–468.

[16] E.C. Gomes, M.A.S. Oliveira, Chemical polymerization of aniline in hydrochloric acid (HCl) and formic acid (HCOOH) media. Differences between the two synthesized polyanilines, Am. J. Polym. Sci., 2 (2012) 5–13.

[17] R.L. Razalli, M.M. Abdi, P.M. Tahir, A. Moradbak, Y. Sulaiman, L.Y. Heng, Polyaniline-modified nanocellulose prepared from Semantan bamboo by chemical polymerization: preparation and characterization, RSC Adv., 7 (2017) 25191–25198.

[18] H.B. Gu, S.B. Rapole, J. Sharma, Y.D. Huang, D.M. Cao, H.A. Colorado, Z.P. Luo, N. Haldolaarachchige, D.P. Young, B. Walters, S.Y. Wei, Z.H. Guo, Magnetic polyaniline nano-composites toward toxic hexavalent chromium removal, RSC Adv., 2 (2012) 11007–11018.

[19] P.B. Liu, Y. Huang, X. Zhang, Superparamagnetic Fe₃O₄ nanoparticles on graphene–polyaniline: synthesis, characterization and their excellent electromagnetic absorption properties, J. Alloys Compd., 596 (2014) 25–31.

[20] K. Chen, J.Y. He, Y.L. Li, X.G. Cai, K.S. Zhang, T. Liu, Y. Hu, D.Y. Lin, L.T. Kong, J.H. Liu, Removal of cadmium and lead ions from water by sulfonated magnetic nanoparticle adsorbents, J. Colloid Interface Sci., 494 (2017) 307–316.

[21] M.R. Lasheen, I.Y. El-Sherif, D.Y. Sabry, S.T. El-Wakeel, M.F. El-Shahat, Adsorption of heavy metals from aqueous solution by magnetite nanoparticles and magnetite-kaolinite nanocomposite: equilibrium, isotherm and kinetic study, Desal. Wat. Treat., 57 (2016) 17421–17429.

[22] P.U. Shah, N.P. Raval, N.K. Shah, Cadmium(II) removal from an aqueous solution using CSCMQ grafted copolymer, Desal. Wat. Treat., 57 (2016) 28262–28273.

[23] C.Y. Li, Y.Y. Yan, Q.Z. Zhang, Z.B. Zhang, L.H. Huang, J.X. Zhang, Y.Q. Xiong, S.Z. Tan, Adsorption of Cd²⁺ and Ni²⁺ from aqueous single-metal solutions on graphene oxide-chitosan-poly(vinyl alcohol) hydrogels, Langmuir, 35 (2019) 4481–4490.

[24] R.-S. Norouzian, M.M. Lakouraj, Preparation and heavy metal ion adsorption behavior of novel supermagnetic nanocomposite based on thiacalix[4]arene and polyaniline: conductivity, isotherm and kinetic study, Synth. Met., 203 (2015) 135–148.

[25] A. Masoumi, M. Ghaemy, A.N. Bakht, Removal of metal ions from water using poly(MMA-co-MA)/Modified-Fe₃O₄ magnetic nanocomposite: isotherm and kinetic study, Ind. Eng. Chem. Res., 53 (2014) 8188–8197.

[26] S. Tabesh, F. Davar, M.R. Loghman-Estark, Preparation of γ-Al₂O₃ nanoparticles using modified sol-gel method and its use for the adsorption of lead and cadmium ions, J. Alloys Compd., 730 (2018) 441–449.

[27] Y. Zhang, Q. Li, L. Sun, R. Tang, J.P. Zhai, High efficient removal of mercury from aqueous solution by polyaniline/humic acid nanocomposite, J. Hazard. Mater., 175 (2010) 404–409.

[28] Y.-M. Hao, C. Man, Z.-B. Hu, Effective removal of Cu(II) ions from aqueous solution by amino-functionalized magnetic nanoparticles, J. Hazard. Mater., 184 (2010) 392–399.

[29] J. Wang, B.L. Deng, H. Chen, X.R. Wang, J.Z. Zheng, Removal of aqueous Hg(II) by polyaniline: Sorption characteristics and mechanisms, Environ. Sci. Technol., 43 (2009) 5223–5228.

[30] R. Karthik, S. Meenakshi, Removal of Pb(II) and Cd(II) ions from aqueous solution using polyaniline grafted chitosan, Chem. Eng. J., 1 (2015) 168–177.

[31] C. Li, H.D. Duan, X.J. Wang, X. Meng, D.W. Qin, Fabrication of porous resins via solubility differences for adsorption of cadmium (II), Chem. Eng. J., 262 (2015) 250–259.

[32] S.A. Jadhav, S.V. Patil, Facile synthesis of magnetic iron oxide nanoparticles and their characterization, Front. Mater. Sci., 8 (2014) 193–198.

[33] F.A. Dawodu, K.G. Akpomie, Simultaneous adsorption of Ni(II) and Mn(II) ions from aqueous solution unto a Nigerian kaolinite clay, J. Mater. Res. Technol., 3 (2014) 129–141.

[34] K.G. Akpomie, F.A. Dawodu, K.O. Adebowale, Mechanism on the sorption of heavy metals from binary-solution by a low cost montmorillonite and its desorption potential, Alexandria Eng. J., 54 (2015) 757–767.

[35] R. Najam, S.A. Muzaffar, Removal of Cu(II), Zn(II) and Cd(II) ions from aqueous solutions by adsorption on walnut shell-Equilibrium and thermodynamic studies: treatment of effluents from electroplating industry, Desal. Wat. Treat., 57 (2016) 27363–27373.

[36] W.H. Lu, J.H. Li, Y.Q. Sheng, X.S. Zhang, J.M. You, L.X. Chen, One-pot synthesis of magnetic iron oxide nanoparticle-multiwalled carbon nanotube composites for enhanced removal of Cr(VI) from aqueous solution, J. Colloid Interface Sci., 505 (2017) 1134–1146.

[37] N. Kataria, V.K. Garg, Green synthesis of Fe₃O₄ nanoparticles loaded sawdust carbon for cadmium (II) removal from water: regeneration and mechanism, Chemosphere, 208 (2018) 818–828.

[38] S.R. Chowdhury, E.K. Yanful, Kinetics of cadmium (II) uptake by mixed maghemite-magnetite nanoparticles, J. Environ. Manage., 129 (2013) 642–651.

[39] D. Mohan, H. Kumar, A. Sarswat, M. Alexandre-Franco, C.U. Pittman Jr., Cadmium and lead remediation using magnetic oak wood and oak bark fast pyrolysis bio-chars, Chem. Eng. J., 236 (2014) 513–528.

[40] D. Mohan, C.U. Pittman Jr., M. Bricka, F. Smith, B. Yancey, J. Mohammad, P.H. Steele, M.F. Alexandre-Franco, V. Gómez-Serrano, H. Gong, Sorption of arsenic, cadmium, and lead by chars produced from fast pyrolysis of wood and bark during bio-oil production, J. Colloid Interface Sci., 310 (2007) 57–73.

[41] H. Yanagisawa, Y. Matsumoto, M. Machida, Adsorption of Zn(II) and Cd(II) ions onto magnesium and activated carbon composite in aqueous solution, Appl. Surf. Sci., 256 (2010) 1619–1623.

[42] P. Liang, T.Q. Shi, J. Li, Nanometer-size titanium dioxide separation/preconcentration and FAAS determination of trace Zn and Cd in water sample, Int. J. Environ. Anal. Chem., 84 (2004) 315–321.

[43] J. Goel, K. Kadirvelu, C. Rajagopal, V.K. Garg, Cadmium(II) uptake from aqueous solution by adsorption onto carbon aerogel using a response surface methodological approach, Ind. Eng. Chem. Res., 45 (2006) 6531–6537.

[44] J.L. Gong, L. Chen, G.M. Zeng, F. Long, J.H. Deng, Q.Y. Niu, X. He, Shellac-coated iron oxide nanoparticles for removal of cadmium(II) ions from aqueous solution, J. Environ. Sci., 24 (2012) 1165–1173.

[45] S.M. Yu, L. Zhai, Y.J. Wang, X.G. Liu, L.C. Xu, L.L. Cheng, Synthesis of magnetic chrysotile nanotubes for adsorption of Pb(II), Cd(II) and Cr(III) ions from aqueous solution, J. Environ. Chem. Eng., 3 (2015) 752–762.

[46] M.H. Beyki, M.H. Ghasemi, A. Jamali, F. Shemirani, A novel polylysine–resorcinol base γ-alumina nanotube hybrid material for effective adsorption/preconcentration of cadmium from various matrices, J. Ind. Eng. Chem., 46 (2017) 165–174.

[47] X.Q. Xue, J. Xu, S.A. Baig, X.H. Xu, Synthesis of graphene oxide nanosheets for the removal of Cd(II) ions from acidic aqueous solutions, J. Taiwan Inst. Chem. Eng., 59 (2016) 365–372.

[48] S. Mallakpour, F. Motirasoul, Bio-functionalizing of α-MnO₂ nanorods with natural L-amino acids: a favorable adsorbent for the removal of Cd(II) ions, Mater. Chem. Phys., 191 (2017) 188–196.

[49] F.Y. Lyu, H.Q. Yu, T.L. Hou, L.G. Yan, X.H. Zhang, B. Du, Efficient and fast removal of Pb²⁺ and Cd²⁺ from an aqueous solution using a chitosan/Mg-Al-layered double hydroxide nanocomposite, J. Colloid Interface Sci., 539 (2019) 184–193.

[50] S. Lagergren, About the theory of so-called adsorption of soluble substances, Kung Sven. Veten. Hand., 24 (1898) 1–39.

[51] Y.S. Ho, G. McKay, Pseudo-second order model for sorption processes, Process Biochem., 34 (1999) 451–465.

[52] C. Ianăşi, M. Picioruş, R. Nicola, M. Ciopec, A. Negrea, D. Nižňanský, A. Len, L. Almásy, A.-M. Putz, Removal of cadmium from aqueous solutions using inorganic porous nanocomposites, Korean J. Chem. Eng., 36 (2019) 688–700.

[53] Z.W. Wang, X.F. Zeng, X.M. Yu, H. Zhang, Z.J. Li, D. Jin, Adsorption behaviors of Cd^{2+} on Fe_2O_3/MnO_2 and the effects of coexisting ions under alkaline conditions, Chin. J. Geochem., 29 (2010) 197–203.